OLCI Level 2

Algorithm Theoretical Basis Document

Rayleigh Correction Over Land

DOCUMENT REF: S3-L2-SD-03-C15-LISE-ATBD
DELIVERABLE REF: SD-03-C
VERSION: 2.1

Document Signature Table

	Name	Function	Company	Signature	Date
Prepared	R. Santer	Consultant	LISE	Santer	01/07/10
Edited revision	S. Lavender	Project Manager	ARGANS Ltd	S J Lavender Digitally signed by Samantha Lavender DN: cn=Samantha Lavender, o=ARGANS Ltd, ou=Managing Director, email=samantha.lavender@argans.co.uk, c=GB Date: 2010.07.02 01:03:16 +01'00'	
Approved	O. Fanton d'Andon	OLCI Coordinator	ACRI-ST		
Released	S. Lavender	Project Manager	ARGANS Ltd		

Change record

Issue	Date	Description	Change pages
1.0	08/04/2009	Version 1 (PDR delivery)	
2.0	09/04/2010	Version 2 (CDR delivery)	Minor updates
2.1	01/07/2010	Delta CDR delivery	Error estimates: addition of Figure 3 and text within Section 5.

Distribution List

Organisation	To
ESA	Philippe Goryl, Alessandra Buongiorno and Carla Santella
EUMETSAT	Vincent Fournier-Sicre and Vincenzo Santacesaria
CONSORTIUM PARTNERS	ARGANS, ACRI-ST, RAL, Brockmann Consult, Elsag-Datamat

Table of Contents

List of Figures

List of Tables

1. INTRODUCTION

The Bottom of Rayleigh Reflectance (BRR) is a level 2 product over land that can be used in pixel classification. The Rayleigh correction formulation, defined for MERIS, remains pertinent for OCLI. One major improvement should be the use of a DEM of improved spatial resolution, and a smile correction is also simple to introduce.

The Rayleigh correction is based on the use of the Rayleigh atmospheric functions, which are computed as interpolated values within LUTs, and can be simplified, by using neural network approaches.

1.1 Acronyms and Abbreviations

ANN	Artificial Neural Networks
ATBD	Algorithm Theoretical Basis Document
BRR	Bottom of Rayleigh Reflectance
DEM	Digital Elevation Model
LUTs	Look Up Tables
MERIS	Medium Resolution Imaging Spectrometer
MLP	Multilayers Perceptrons
OLCI	Ocean Land Colour Imager
ROT	Rayleigh Optical thickness
RTC	Radiative Transfer Code
SAA	Satellite Azimuth Angle
SOS	Successive Order of Scattering code
SZA	Sun Zenith Angle
TOA	Top of Atmosphere
VAA	Viewing Azimuth Angle
VZA	Viewing Zenith Angle

1.2 Purpose and Scope

BRR can be used to produce land classification maps to start an algorithm for aerosol remote sensing… Therefore an implementation in OCLI is adopted. Using the simple procedure in Section 2, we can determine the BRR from the top of atmosphere (TOA) reflectance. The definition and the basic way to compute the Rayleigh function is described in Section 3. What is done for MERIS is applicable to OCLI Section 4, but improvements can be conducted as indicated in Section 5.

1.3 Algorithm Identification

This algorithm is identified under reference “SD-03-C15” in the Sentinel-3 OLCI documentation.

2. ALGORITHM OVERVIEW

2.1 Theoretical Description

A Simplified formulation of the Rayleigh contribution

Outside of the strong absorption bands (*i.e.*, in the O_2 and H_2O bands), the coupling between scattering and gaseous absorption remains relatively weak. This assumption leads to express the apparent reflectance ρ^* at top of the atmosphere (TOA) as:

$$\rho^* \approx \rho^*_{na} \,.\, T_g \qquad (1)$$

Where ρ^*_{na} is the signal ignoring the gaseous absorption and T_g the gaseous transmittance. The next step is to correct for the well known Rayleigh scattering. To do so, a simplified formulation of the signal will be used followed by an indication of how the different Rayleigh scattering functions were computed. Then, we will illustrate the limitations of this Rayleigh correction.

A simple two-layer model shows a schematic representation of the atmosphere l: molecules over aerosols. The spectral dependency of the *Rayleigh* optical thickness is well known. This optical thickness is proportional to the barometric pressure (P) at the ground surface. The geometry of the observation is described by the solar and viewing zenithal angles, respectively ϑ_s and ϑ_v (or the cosine of this zenith angle μ), and by the difference in azimuth φ. Thus, the *Rayleigh* contribution above the aerosol-ground system can be written, following the 6S code formulation, Vermote et al. (1997), as:

$$\rho^*_{na} = \rho_R + T_R(\mu_s) \, . \frac{\rho_{aG}}{1-\rho_{aG} \, . S_R} \, . T_R(\mu_v) \qquad (2)$$

where ρ^*_{na} is the apparent reflectance at TOA (corrected for gaseous absorption), ρ_R the *Rayleigh* reflectance, ρ_{aG} the aerosol-ground system reflectance, $T_R(\mu_s)$ and $T_R(\mu_v)$ the downward and upward *Rayleigh* transmittance respectively and S_R the spherical albedo relating to the molecules.

There are two basic assumptions contained in equation (2):

(i) On the vertical distribution: the molecular layer is put above the aerosol layer.

(ii) On the bi directionality of the radiances at the top of the aerosol layer. The BRR (bottom of Rayleigh) is assumed to be Lambertian.

According to Equation 2, we can easily correct for *Rayleigh* scattering to retrieve the reflectance above the aerosol-ground system. First, if we ignore the coupling between reflection *and scat*tering:

$$\rho^C_{aG} = (\rho^*_{na} - \rho_R) / T_R(\mu_s) \, . T_R(\mu_v) \qquad (3)$$

Second, after correction of this term:

$$\rho_{aG} = \frac{\rho^C_{aG}}{1+\rho^C_{aG} \, . S_R} \qquad (4)$$

Definition and computation of the Rayleigh scattering functions

Standard values of the Rayleigh optical thicknesses

The *Rayleigh* optical thickness, ROT, $\tau_R^j(\lambda, P_0)$ is estimated for each OCLI band *j* (*Hansen and Travis*, 1974); λ is the nominal central wavelength and the pressure P_{std} is the standard pressure (1012 *hPa*).

λ	*412.50*	*442.50*	*490.00*	*510.00*	*560.00*	*620.00*	*665.00*
τ_R	0.315280	0.235910	0.155155	0.131714	0.089912	0.059433	0.044730

λ	*681.25*	*708.75*	*753.75*	*778.75*	*865.00*	*885.00*
τ_R	0.040562	0.034558	0.026944	0.023617	0.015459	0.014099

Table 1: Rayleigh optical thickness in 13 MERIS spectral bands.

The Fourier series expansion of the radiation field

Most of the radiative transfer codes (RTC) use a Fourier series expansion of the radiation field as:

$$\tilde{L}_R(\vartheta_s, \vartheta_v, \Delta\phi) = \sum_{s=0}^{2} (2 - \delta_{0,s}).\tilde{L}_R^{(s)}(\vartheta_s, \vartheta_v).\cos(s.\Delta\phi) \tag{5}$$

For the Rayleigh scattering, the Stokes vector $\tilde{L}_R$ is expanded in three Fourier terms $\tilde{L}_R^s$ (s=0,1,2). $\vartheta_s, \vartheta_v, \Delta\phi$ are respectively the solar zenith angle, the view zenith angle, the difference in azimuth; $\delta_{0,s}$ is the *Dirac*'s function.

Rayleigh primary scattering

In the near infrared, the primary scattering regime dominates. The incident solar light is unpolarized. For the primary scattering, the Stoke vector is reduced to the radiance, or to the reflectance. At TOA, we express the Rayleigh reflectance for the 3 Fourier series terms as the product of the Rayleigh phase function by a term depending on the geometry and on the ROT.

$$\rho_{R,P}^{(s)}(\vartheta_s,\vartheta_v,\tau^R) = P_R^{(s)}(\vartheta_s,\vartheta_v)\,.\,\frac{(1-e^{-M.\tau_R})}{4\,.(\cos\vartheta_s+\cos\vartheta_v)} \quad (6)$$

with, M , the air mass defined as:

$$M = \frac{1}{\cos\vartheta_s}+\frac{1}{\cos\vartheta_v} \quad (7)$$

The Fourier series expansion of the Rayleigh phase function

$P_R^{(s)}$ the *Rayleigh* phase function for each *Fourier* series term s is independent on the wavelength and expressed as:

$$\begin{cases} P_R^{(0)}(\vartheta_s,\vartheta_v) = \dfrac{3A}{4}.\left(1+\cos^2\vartheta_s\,.\cos^2\vartheta_v+\dfrac{\sin^2\vartheta_s\,.\sin^2\vartheta_v}{2}\right)+B \\ P_R^{(1)}(\vartheta_s,\vartheta_v) = -\dfrac{3A}{8}.\cos\vartheta_s\,.\cos\vartheta_v\,.\sin\vartheta_s\,.\sin\vartheta_v \\ P_R^{(2)}(\vartheta_s,\vartheta_v) = \dfrac{3A}{16}.\sin^2\vartheta_s\,.\sin^2\vartheta_v \end{cases} \quad (8)$$

with $A = 0.9587256,\ B = 1-A$

A and B are the coefficients which account for the molecular asymmetry

The successive order of scattering and the Rayleigh reflectance

The Rayleigh scattering is computed using the successive order of scattering code (SOS), *Deuzé et al. (1989)*. The code solves the radiative transfer equation in the vector mode.

Simulations underline the need to account for the polarization in the Rayleigh reflectance computations (*Santer et al, 2002*). If not, relative errors as high as 6 percent can be made.

We introduce a multiplicative function $f_R^{(s)}$ which accounts for the multiple scattering. Thus the *Rayleigh* reflectance $\rho_R^{(s)}$ for each *Fourier* series term s is written as:

$$\rho_R^{(s)}(\vartheta_s, \vartheta_v, \tau^R) = \rho_{R,P}^{(s)}(\vartheta_s, \vartheta_v, \tau^R) \,.\, f_R^{(s)}(\vartheta_s, \vartheta_v, \tau^R) \qquad (9)$$

where $\rho_{R,P}^{(s)}$, the primary scattering reflectance for *Rayleigh.*

What are the advantages of these different decompositions:

(i) The Fourier series expansion has only 3 terms.

(ii) The primary scattering has a simple analytical formulation.

(iii) The multiplicative function $f_R^{(s)}$ can be fitted by a polynomial of order 2.

The Rayleigh transmittances

The *Rayleigh* transmittance applies both on the downward and upward paths. Following the principle of reciprocity, it is the same function depending only on the zenith angle.

A quite accurate formulation is available in the 6S code (*Vermote et al.*, 1997):

$$T_R^{6S}(\tau_R, \mu) = \frac{(2/3+\mu)+(2/3-\mu).e^{-\tau_R/\mu}}{(4/3+\tau_R)} \qquad (10)$$

The transmittance is defined as the ratio between the downwelling total irradiance (direct +diffuse) at the surface to the incident solar irradiance at TOA. In the SOS code, the solar irradiance at TOA is normalized to π.

$$T_R^{SOS}(\tau_R, \mu) = \exp(-\tau_R/\mu) + \phi_R^d(\mu, \tau_R)/\mu\pi \qquad (11)$$

The computation of the diffuse irradiance $\phi_R^d(\mu, \tau_R)$ requires only the Fourier series term s=0 with:

$$\phi_R^d(\mu,\tau_R)=2\pi.\int_0^1 L_R^{s=0}(\tau_R,\mu,\mu').\mu'.d\mu \quad (12)$$

In the SOS code, the angular integration is made with 24*2 Gaussian angles (*2 for up and down). The Gaussian quadrature is applied to Eq. (12):

$$\phi_R^d(\mu,\tau_R)=2\pi.\sum_{j=1}^{24} L_R^0(\mu,\mu_j,\tau_R)w_j \quad (13)$$

μ_j and w_j are respectively the cosine and the weight of the 24Gausian angles.

The Rayleigh spherical albedo

The *Rayleigh* spherical albedo (S_R) is defined as

$$S_R(\tau_R)=1-2.\int_0^1 T_R(\tau_R,\mu).\mu.d\mu \quad (14)$$

Using the Gaussian quadrature:

(i) $T_R(\mu,\tau_R)$ is computed with the SOS code for 24 Gaussian angles as solar zenith angle and s=0.

(ii) Using the Gaussian quadrature, Eq. (14) is rewrite as:

$$S_R(\tau_R)=1-2.\sum_{j=1}^{24} T_R(\tau_R,\mu_j)w_j \quad (15)$$

2.2 MERIS like computation and associated LUTs

Grid for Rayleigh computation

The Rayleigh scattering functions are computed at the centre of a 4*4 pixels grid in which we know the:

(i) geometrical conditions: SZA, VZA, SAA, VAA.

(ii) sea level pressure P_o.

(iii) The surface elevation *z*.

Rayleigh phase function computation

We first compute the scattering angle Θ. The Rayleigh phase function is expressed as:

$$P_R(\Theta)=3A(1+\cos^2(\Theta))/4+B \tag{16}$$

with $A=0.9587256,\ \ B=1-A$

Rayleigh optical thickness computation

The ROT τ_R^j for the 13 MERIS nominal bands *j* are in a LUTs. They are corrected by the barometric pressure at the surface elevation with:

$$P(z)= P_o \exp(-z/8000) \tag{17}$$

according to the molecular scale height of 8 000 m, if z is in metres.

Eq. (17) is an approximation which needs to be revisited. The temperature at surface level is an additional parameter to *z* to trigger the altitude correction from the sea level pressure to the surface pressure.

For the window, the ROT are weighted by the pressure with:

$$\tau_R^{(j)}(P_o,z)=P(z)*\tau_R^j/P_{std} \tag{18}$$

Rayleigh primary scattering computation

The reflectance is computed following:

$$\rho_{R,P}^j=P_R(\Theta).\frac{(1-\exp(-M*\tau_R^j))}{4.(\cos\vartheta_s+\cos\vartheta_v)} \tag{19}$$

The wavelength dependence is contained in τ_R^j.

Rayleigh reflectance computation

The multiplicative *Rayleigh* scattering functions $(f_R^{(s)})$, determined for each of the first 3 *Fourier* series terms (s), have been expanded as:

$$f_R^{(s)}(\vartheta_s,\vartheta_v,\tau_R)=\sum_{i=0}^{3}k_i^{(s)}(\vartheta_s,\vartheta_v).(\tau_R)^i \qquad (20)$$

with $k_i^{(s)}$ the polynomial coefficients for the *Fourier* series term s. $k_i^{(s)}$ are pre-computed in LUT for s=0,1,2 and 12 Gaussian angles. A double linear interpolation (in SZA and VZA) to produce $k_i^{(s)}(\theta_s,\theta_v)$

In a loop on the 13 MERIS bands, we then compute $f_R^{(s)}(\vartheta_s,\vartheta_v,\tau_R^j)$. The *Rayleigh* scattering function (f_R^j) will be then computed by recombining the first 3 *Fourier* series terms as follows:

$$f_R^j(\vartheta_s,\vartheta_v,\Delta\phi)=\sum_{s=0}^{2}(2-\delta_{0,s}).f_R^{(s)}(\vartheta_s,\vartheta_v,\tau_R^j).\cos(s.\Delta\phi) \qquad (21)$$

Finally, the Rayleigh reflectance is:

$$\rho_R^j = f_R^j(\vartheta_s,\vartheta_v,\Delta\phi)\ \rho_{R,P}^j \qquad (22)$$

Rayleigh transmittance computation

For the 13 MERIS bands, the *Rayleigh* transmittance (T_R) is estimated with a second order polynomial function of the *Rayleigh* transmittance derived from the 6S model (T_R^{6S}), see Eq. (10):

$$T_R(\tau_R,\mu_s)=\sum_{i=0}^{2} t_i.\left(T_R^{6S}(\tau_R,\mu_s)\right)^i \qquad (23)$$

Where μ_s is the cosine of solar zenith angle (ϑ_s) and τ^R *is* the *Rayleigh* optical thickness. The t_i polynomial coefficients (LUT074). This computation applies as well to the upward path (μ_v instead of μ_s).

Rayleigh spherical albedo computation

Eq. (15) is used to generate the spherical albedo with ROT between 0.02 and 0.32 with a step of 0.02.The details on the MERIS computations are available from the MERIS Level-2 detailed processing model (*MERIS L2 DPM*, 2005).

The LUTs

The details on the MERIS LUTs are available in (*Zagolski et al*, 2005) and the Rayleigh LUTs are described in Table 2.

Table 1 is LUT097. The other LUTs have been generated with the SOS code using the 24 Gaussian angles of LUT080. To save space and time, a subset of 12 Gaussian angles has been selected (2.84, 17.63841, 28.76843, 36.18973, 43.61145, 51.03339, 58.45547, 65.87766, 69.58877, 73.29988, 77.01101 and 80.72215). With the symmetry (*θs, θv)*, the scattering coefficients f (LUT101) are produced for 78 pairs of zenith angles (LUT081).

The three transmittance coefficients have been produced from the computation by the SOS code of $T_R^{SOS}(\tau_R,\mu=1)$ for a sun at zenith and 17 ROTs. The limitation at *θs* =0° needs to be evaluated. The larger value of the ROT is 0.32 with corresponds to 412 nm. The selection for OCLI of a band at 400 nm will impose to add two values (0.34 and 0.36). The smaller value of the ROT is 0.02, which means that B13 and B14 are already extrapolated. It certainly relevant to add ROT=0 in the LUTs. It will give:

(i) verify (or impose) $k_0^{(s)}$ =0

(ii) verify (or impose) t_0 =0

(iii) impose $S_R(\tau_R=0)=0$

Acronym	Name	Content	Size
LUT097	*optical thickness*		13
LUT080	Θ		24
LUT081	$\theta s \times \theta v$		78
LUT101	*rayscatt_coef*	$f[s, \theta s \times \theta v, k]$	3*78*3
LUT074	*transmittance coefficient*	t0, t1, t2	3
LUT102	*spherical albedo*		17

Table 2: The Rayleigh LUTs

2.3 Algorithm Validation

To be completed in a future issue of this document.

3. ASSUMPTIONS AND LIMITATIONS

The Baseline is the MERIS-like algorithm, with a better DEM, in order to keep it out of the critical path. Alternatively, the O2 surface pressure can be used to replace the ECMWF pressure combined with the DEM improvement. An future evolution is the use of Neural Networks to replace the interpolations made on the grid points of the LUTs.

3.1 Limitation of the MERIS like approach and recommendations for OCLI

The smile effect

It is possible to simply include the smile correction with:

$$\tau_R^{(j)}(P_o, z, i) = \tau_R^{(j)}(P_o, z)(\lambda_j^i / \lambda_j^n)^{-4} \qquad (24)$$

is the nominal wavelength for band j, λ_j^i is the effective wavelength for band j and for pixel i. For MERIS, the amplitude of the smile is 1 nm. In the blue, the smile effect impacts the ROT by one percent. It is small but when it is possible to correct it …

Resolution of the DEM

In BEAM, it is possible to use a DEM with a resolution of 1 km (getasse option). Using Eq. (7), we compute the pressure with the MERIS DEM and this high resolution DEM. We illustrate in Figure 1 the two possibilities. Clearly, over mountains, the current MERIS DEM does not offer the required surface pressure.

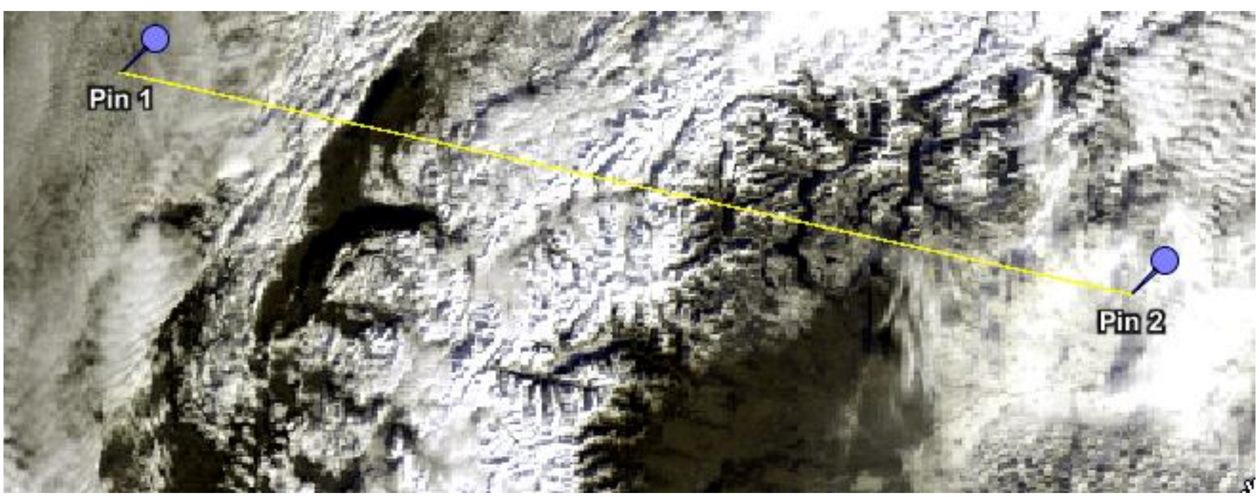

(a)

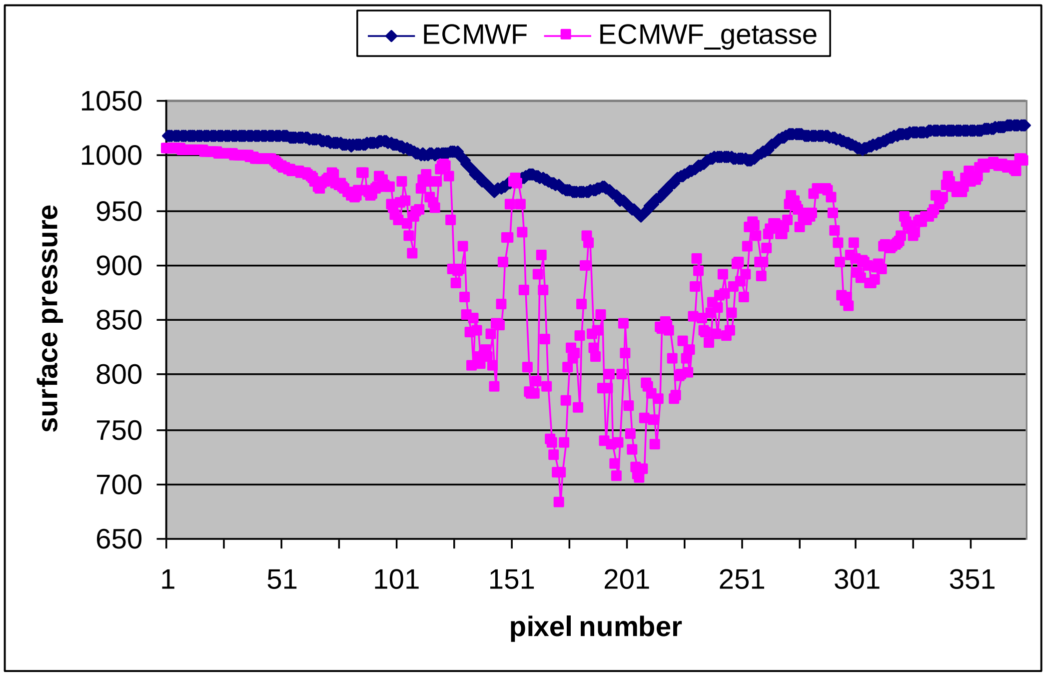

(b)

Figure 1: (a) RGB MERIS image of the Alps and a selected transect: (b) Surface pressure (hPa); Comparison between the regular MERIS and using a high resolution DEM.

A better DEM is required and key information can be derived as well from a high resolution DEM as soon as the geo localisation is satisfactory. The terrain slope is an indicator on the validity of the conversion of radiance to reflectance. This conversion assumes the surface to be horizontal in mean in the pixel. The dream is to have an accurate surface pressure derived from the oxygen band(s?) in the Rayleigh computation.

Use of the O_2 derived surface pressure

MERIS has two spectral bands (B10 and B11) to derive over land the surface pressure. At the very beginning, this O_2 surface pressure was planned to be used in two ways:

(i) In the pixel classification to detect the presence of semi transparent clouds such as cirrus clouds.

(ii) To compute the Rayleigh optical thickness.

The poor quality of the surface pressure product resulted in the de-scoping of its involvement in the two tasks. Through the ongoing O_2 project, substantial improvements have been made on this MERIS O_2 surface pressure. For OLCI, we will have an additional spectral band in the O_2 absorption lines and therefore we can expect to even have a better determination.

Replace the LUTs by a neural network.

A good way to approximate the radiative transfer is to use artificial neural networks (ANN). A particular class of ANN, the so-called multilayers perceptrons (MLP), was used by *Brajard et al, 2009*, to simulate the atmospheric reflectance transmittance in the MERIS bands over water. One MLP is dedicated to the simulation of ρ_{atm} (denoted MLP-A), and one to T (MLP-T). A sub-dataset of 150 000 ρ_{atm} (resp. T) was randomly extracted from LUT-A (resp. LUT-T) to calibrate MLP-A (resp. MLP-T). Figure 2 is a representation of the MLP.

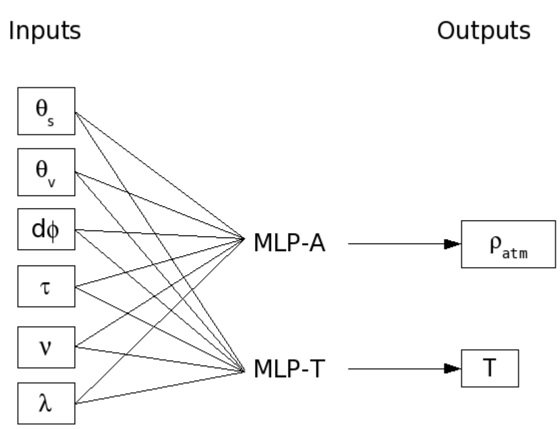

Figure 2: Representation of the two MLPs used to simulate the direct model.

This approach is simplified for the Rayleigh. Only (ϑ_s), (ϑ_v), $(d\phi)$ and (τ^R) are the inputs for the MLP for the reflectance. Only (ϑ_s), (or (ϑ_v)) and (τ^R) are the inputs for the MLP for the transmittance. It will be faster and more accurate than the previous approach, and also simpler to code it.

4. INPUT DATA

Geometry including illumination and viewing zenith and azimuth angles: θ_s [degrees], θ_v [degrees] and $d\phi$ [degrees]

Apparent reflectance at TOA (corrected for gaseous absorption): ρ^*_{na} [dimensionless]

DEM: Digital Elevation Model [m] from external source

5. ERROR BUDGET

Assuming that:

(i) the smile effect is corrected

(ii) the good accuracy of the DEM and it good spatial

The key input is the barometric pressure and the error impact can be simply evaluated from the 6S formulation, see equation 3. To some extent, because the production of the land surface reflectance does not account for aerosols, an error budget is of lower importance.

In order to give an idea on the error, we compute the TOA signal for a pure molecular atmosphere, a nadir view and a solar angle of 60 degrees for three surface albedos: 0.15, 0.3 and 0.5. The signal was computed for a pressure of 1007 hPa and inverted with 1012 hPa. The results are reported in absolute error on albedo (in percentage) on figure 3.

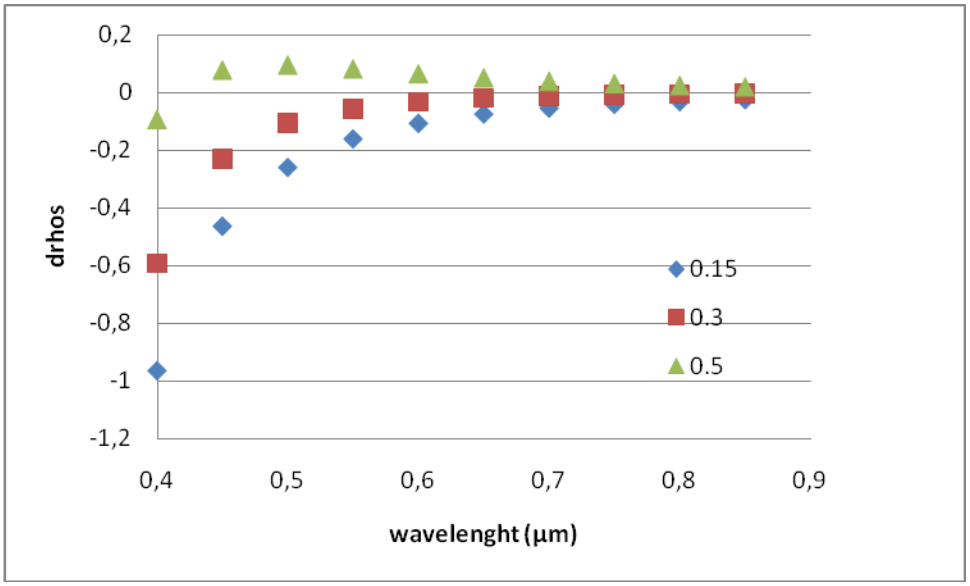

Figure 3: Absolute error on the retrieval of the Bottom of Rayleigh Reflectance (in percent) versus the wavelength for 3 "white" values of the surface albedo. Error on the barometric pressure is 5 hPa.

If we want to estimate the error, the simple way to implement the error bar is to do two Rayleigh corrections: one with the nominal pressure and the second by adding an error on it (nominal is 5 hPa). Alternatively, we can to the first order compute the correction based on the Rayleigh functions:

The Rayleigh computation of the optical thickness τ_R^0, of the reflectance ρ_R^0 and of the transmittances total T_R^0 are conducted for the ECMWF surface pressure P_0 and we used a pressure $P = P_0$ +*dP* to evaluate the error. We directly have:

$$d\tau_R = \tau_R^0 \, dP \; / P_0 \qquad (25)$$

$$d\rho_R = \rho_R^0 \, dP \; / P_0 \qquad (26)$$

$$T_R = T_R^0 \exp(-0.5 * d\tau_R / \mu) \qquad (27)$$

And with these corrected Rayleigh functions, we use again Eq. (3) to get a second value of the surface reflectance to determine the error bar.

6. REFERENCES

Aubertin, G., and J.F. Leroux, 2000: "Software user's manual for MERIS Level-2 auxiliary data tool software*", ABB-BOMEM report (PO-MA-BOM-GS-0008)*, Quebec (Qc): 50 p.

Brajard J., Santer R., Crépon M., Thiria, S. "Atmospheric correction of MERIS data for case 2 waters". Submitted in Remote Sensing of Environment, January 2009.

Deuzé, J.L., M. Herman and R. Santer, 1989**:** "Fourier series expansion of the transfer equation in the atmosphere-ocean system", *J. Quant. Spectroscop. Radiat. Transfer.*, 41 (6): 483-494.

Hansen J and Travis D., 1974. "Light scattering in planetary atmospheres", *Space Science Reviews*: **16**, 527-610.

Santer, R., V. Carrere, P. Dubuisson and J.C. Roger, 1999**:** "Atmospheric corrections over land for MERIS", *Int. J. Remote Sensing*, 20 (9): 1819-1840.

Santer R., Fischer J., Zagolsky F., Ramon D. and Dubuisson P. (2002). Uncertainties in radiative transfer computations. Consequences on the MERIS products over land. *Proceedings of SPIE. Optical Remote Sensing of the Atmosphere and Clouds III. Editor(s): Hung-Lung Huang, Daren Lu, Yasuhiro Sasano, Vol. 4891, p. 150-160.*

Vermote E., Tanré D., Deuzé J. L., Herman M and Morcrette J. J., 1997 : "Second Simulation of the Satellite Signal in the Solar Spectrum, 6S: An overview." *IEEE Transactions on Geoscience And Remote Sensing,* **35**, 3, 675-686.

Zagolski F., Aubertin, G., J.F. Leroux, Péron G,.2005, Specification of the Scientific Contents of the MERIS Level 2 Auxiliary Data Product, *BOMEN report,* PO-RS-BOM-GS-0002, 30 Nov 2005